IV.1. Iron Fischer-Tropsch Catalyst. A Study of the Oxidation of Ferrous Hydroxide in Slightly Basic Solution to Produce γ-FeOOH. (R. Lin, R. Spicer, F. L. Tungate and B. H. Davis).

IV.1.1. ABSTRACT

During the reaction of Fe(II) with oxygen, three regions of nearly constant pH are observed, each separated by two regions where there is an abrupt pH change. Data for the oxidation of a suspension with $[Fe(II)]/[OH^-] = 7/12$ and 0.22M Fe(II) indicate that the oxidation to Fe(III) and the associated hydrolysis to produce a proton are rapid compared to the reaction that consumes the proton generated during the first step. It is suggested that the oxidation occurs in the aqueous solution, and that the slow step is due to the proton reacting with a solid Fe(II) species to produce soluble Fe(II). Fe_3O_4 is formed at, or near, the first step in the oxidation-pH curve, and then redissolves as oxidation continues. The amount of Fe(II) and Fe(III) in the solid and solution have been determined at several stages of the oxidation, and these are consistent with the amount of oxygen consumed during the reaction.

IV.1.2. INTRODUCTION

The aerial oxidation of $Fe(OH)_2$ in aqueous solution can produce Fe_3O_4, α-FeOOH or γ-FeOOH; the compound obtained depends on the reaction temperature, oxidation rate, initial concentration of the reactants and pH of the solution. Recently, it was reported that the initial molar ratio, $[Fe(II)]/[OH^-] = R$, significantly affected the structure of the product obtained by the air oxidation of $Fe(OH)_2$ (IV.1.1). For example, γ-FeOOH was the major product when $R = 0.5833$ (7/12) but it was not formed when $R < 0.5$.

On the other hand, it was reported that aerial oxidation of a neutral or slightly alkaline suspension containing $Fe(OH)_2$ yielded an intermediate green complex and solid Green Rust I or II (GRI or GRII), depending on the anion added to prepare the suspension. Green Rust I was formed when $FeCl_2$ was used as the starting material while Green Rust II was obtained when $FeSO_4$ was used. The formation of Green Rust as an intermediate is considered to be necessary if γ-FeOOH is the desired product (IV.1.2-IV.1.5). GR contains both Fe(II) and Fe(III) although its chemical composition has not been exactly defined. GR can be further oxidized by air or oxygen to form either Fe_3O_4 or γ-FeOOH, or a mixture of the two, depending on the oxidation rate. Fast oxidation produces γ-FeOOH while slow oxidation results in the formation of Fe_3O_4. Therefore, the formation of γ-FeOOH is restricted to the instances where the rapid aerial oxidation of ferrous ion is effected in a neutral or slightly basic suspension of $Fe(OH)_2$. However, γ-FeOOH is not formed by the addition of a base to effect precipitation of iron from a solution prepared from a ferric salt.

Although the oxidation of $Fe(OH)_2$ has been studied by several groups, many questions still need to be answered about the mechanism of the formation of γ-FeOOH. In addition, the procedure for the synthesis of pure γ-FeOOH on a large scale has not been well defined. This study is to an attempt to define better the chemistry associated with the oxidation of Fe(II) to γ-FeOOH, and to provide a rationale for scaling this method up to produce kg/hr or larger amounts of γ-FeOOH.

IV.1.3. EXPERIMENTAL

Materials: Melanterite ($FeSO_4 \cdot 7H_2O$), NaOH and $Fe_2(SO_4)_3$ were purchased from Aldrich. The chemicals were ACS reagent grade and were stored in a desiccator to prevent deterioration.

Apparatus: A four-neck round-bottom flask (1L) was fitted with a gas disperser (fritted-glass disc), pH electrode, motor-driven stirrer and gas inlet/outlet tubes. Inlet gas flow rate was monitored by a rotameter and the outlet gas by a wet-test flowmeter. The reaction vessel was placed in a constant-temperature water bath.

IV.1.3.a. Preparation and Methods

After adding 750 mL deionized water to a 1L reaction flask, nitrogen gas was bubbled through the water (stirred at 800 r.p.m.) for 40 min to remove dissolved carbon dioxide and oxygen, and then 41.7 g of $FeSO_4 \bullet 7H_2O$ was added. After 10 minutes, solid NaOH (10.3 g) was added to give a molar ratio of [Fe(II)] / [OH^-] of 0.5833 (= 7/12). The suspension was stirred for 15 minutes under nitrogen at room temperature until the suspension pH became constant. Oxygen was then passed into the solution at a constant rate of 18.5 cm^3/min. Reaction time was measured from the start of oxygen flow. During the reaction, the pH value was recorded every minute. The extent of the oxidation reaction was easily recognized from a comparison of the outlet and inlet flow rate of oxygen, the pH of the suspension and the color. After 1 hr the oxidation had essentially stopped. The product was then collected by filtration and then washed with deionized water several times until SO_4^{2-} was not detected in the filtrate. A $BaCl_2$ solution was used to test for the presence of SO_4^{2-}. The filter cake

was then washed with acetone to remove most of the water. The precipitate was dried in vacuum at room temperature for 24 hr.

The X-ray diffraction pattern of the product was measured using Cu K_α (1.5418 Å) radiation (40 KV and 20 mA) with a Philips X-ray diffractometer. For analysis by X-ray diffraction, the solid sample was ground and placed in a sample holder in a glovebox. The sample was removed from the glovebox immediately prior to the measurements.

To determine the phase and chemical composition of the intermediate products, samples were taken at increasing time intervals and transferred to a Schlenk filter tube by a syringe; this was accomplished without exposure to air. The solid was collected and then washed successively with deoxygenated water and acetone, dried in vacuum at room temperature and stored at 4°C under a nitrogen atmosphere. For analysis by X-ray diffraction, the material was placed in a sample holder in a glovebox immediately before recording the diffraction pattern. The identification of the product was accomplished by matching the diffraction peak position and intensity with standards contained in the ASTM data (IV.1.1,IV.1.6).

An experiment was conducted so that samples could be collected at various stages of the synthesis without exposure to oxygen. For the preparation of the $Fe(OH)_2$ suspension, 1.5L deionized water was added to a 2L of reaction flask, nitrogen gas was bubbled into the water while it was being stirred at 800 rpm for 40 minutes to remove O_2 and CO_2, and then 100g of $FeSO_4 \bullet 7\ H_2O$ was added to produce 0.22 M solution. After 10 minutes, 24.67g of NaOH was added to the solutions to give a molar ratio of [Fe(II)] : [OH] of 0.5833 (7/12). The suspension was

stirred for 15 minutes under nitrogen at room temperature until the suspension pH became constant. Oxygen was then passed at a constant rate of 18.5 mL/min through the suspension. Reaction time was measured from the beginning of oxygen flow. During the reaction the pH was measured every minute.

During the course of the oxidation, samples were removed at appropriate intervals. To determine the extent of oxidation, samples of the slurry were withdrawn without exposure to oxygen and quenched in H_2SO_4 (2N). Both iron (II) and the total iron content were determined by titration with $KMnO_4$. To obtain the phase and composition of the intermediate solid products that were found during the oxidation, 60 mL of the suspension was removed by a syringe and transferred to a Schlenk filter tube. The sample was flushed immediately with ultra-pure nitrogen to stop the oxidation. After 10 minutes, nitrogen flow was stopped and the filter tube was sealed by a rubber septum. The solid was collected, then washed twice with 50mL of cool, distilled, deoxygenated water, dried in a vacuum at room temperature, and stored in the Schlenk tube at 4°C. These operations were carried out under nitrogen. The filtrate was collected directly into a 250 mL flask which has been filled with ultra-pure nitrogen, sealed with a rubber septum and stored under nitrogen at 4°C.

To determine the Fe(II) and total iron contents of the solid intermediate products, the Schlenk filter tube, which contained the solid sample, was opened in a glovebox. A known portion of the sample was transferred to a conical beaker containing 2N degassed H_2SO_4, the solid was dissolved by heating, and then cooled to room temperature. The conical beaker was sealed under a rubber septum, and removed from the glovebox. The iron (II) and total iron in the sample was determined

for aliquots of the sample. Fe(II) was obtained from titrating one aliquot and total iron was obtained by titrating the other aliquot after the Fe(III) had been reduced to Fe(II) using metallic zinc. A portion of the filtrate was removed from the glovebox and analyzed for Fe(II) and total iron in a similar procedure. Within analytical error, the iron (II) content in the filtrate was equivalent to the total iron content.

IV.1.4. RESULTS

A white precipitate was formed when $FeSO_4$ and NaOH were mixed in a ratio that produced a suspension with a pH of 8.2. When oxygen was passed through the resulting iron(II) hydroxide suspension, the white precipitate was oxidized and the color of the mixture turned first to green, then blue, and finally orange-yellow. Oxygen was completely converted when its flow rate was 18.5 mL/min (Figure IV.1.1); oxygen usage can be easily estimated from the oxygen flow data. Approximately one hour was needed to complete the conversion of 6/7th of the Fe(II) to Fe(III).

The change in pH with time during the oxidation process is presented in Figure IV.1.1. At least two stages can be observed. During the first stage, the pH of the suspension was reduced only from 8.2 to about 8.0. The viscosity of the mixture increased as oxidation progressed during this first stage. The first stage took about 16 min. during which approximately 28 mol% of the total iron(II) was oxidized. At the end of this stage, the pH abruptly decreased to about 6.5 during 4-5 min with continuous oxygen flow. During this time, however, the pH did not continue to decrease if the oxygen flow was stopped. Thus, the sharp drop in pH is due to oxidation of Fe(II) by oxygen, and the hydrolysis reactions of the oxidation species.

During the second stage of oxidation the pH remained at 6.5. When oxygen flow was stopped at any time during this second stage, the pH of the suspension increased slightly to about 7.0. However, the pH quickly decreased to 6.5 when oxygen flow was resumed. As with the first stage, there was finally an abrupt decrease in pH to less than 4. Following the second abrupt decrease in pH, oxygen consumption became very low and the pH remained nearly constant. The second step occurred when about 85 mole % of the total Fe (II) had been oxidized to Fe(III).

It should be possible to mimic the oxidation process by stopping the oxygen flow and adding Fe(III). This experiment is illustrated in Figure IV.1.2. Oxygen flowed through the suspension during the period corresponding to the portion of the curve between A and B. At B, the pH had just started to decrease corresponding to completion of the first stage. At this point the oxygen flow was stopped and a slight increase in the pH occurred (BC). At point C, a solution of Fe(III) sulfate was added at a rate to correspond to a rate of Fe(III) being formed had oxygen flow continued. The Fe(III) caused the pH to decrease just as oxidation to Fe(III) does; this means that the hydrolysis, or other reactions, of the Fe(III) ion is responsible for the generation of H^+. At the second stage, however, the addition of Fe(III) had only a transitory impact upon the pH/time curve. The addition of Fe(III) does not appear to influence the time required to complete the second stage of the oxidation. In Figure IV.1.1 it is noted that the time required to complete the first stage is about half that required for the second stage; this is expected if the green rust has a stoichiometry corresponding to $\{Fe(III)_2\ Fe(II)_4\ (FeSO_4)\}^{14+}$. In Figure IV.1.2, it appears that the

times required for each of the stages is similar to that of Figure IV.1.1 if the time when oxygen is not flowing is taken into account.

The results in Figure IV.1.3 demonstrate the impact of stopping oxygen flow for a period and for adding H_2SO_4 (2N) at a rate that would correspond to the conversion of oxygen to produce H^+. In the experiment represented in Figure IV.1.3, oxygen flow was continued until the pH began to decline (portion AB). At point B the oxygen flow was terminated and there was a gradual, but slight, increase in pH (BC). The slow increase in pH implies that the rate of production of H^+ is more rapid than the reactions(s) which consume H^+. One possibility is that the dissolution of $Fe(OH)_2$ is the proton consuming reaction:

$$Fe(OH)_2 + H^+ \rightarrow FeOH^+ + H_2O \qquad \text{[IV.1.1]}$$

At point C, sulfuric acid was added at a rate corresponding to that of the oxidation due to the flowing oxygen; the pH changed just as it did in Figure IV.1.1 for oxidation with O_2. The addition of sulfuric acid during the second stage (at points D, E and F) caused a decrease in the pH. However, in the absence of a flow of oxygen the pH, following sulfuric acid addition, gradually returned to about the same pH as before addition of the acid. This is again consistent with the reaction that consumes H^+ being a slow reaction. The addition of H_2SO_4 during either stage one or stage two had only a transitory impact upon the pH/time curve.

The addition of base during the second stage caused an immediate increase in pH (Figure IV.1.4). Continuing the oxygen flow following base addition caused a rapid decrease in pH. This again implies that H^+ generation during oxygen addition is

rapid, and that H^+ reaction with OH^- is rapid compared to the gradual reaction of the H^+ generated or added under conditions shown in Figure IV.1.3.

The oxidation of $FeSO_4$ has also been carried out in a dilute solution. A $FeSO_4$ solution (0.029M, 750 ml) was carefully titrated with NaOH (0.1N) until the pH of the solution was 7.8; precipitation did not occur during this operation. Oxygen was then passed through this solution at a flow rate of 18.5 mL/min. The pH vs. time curve (Figure IV.1.5) shows that an obvious plateau for the first stage is not detected; instead, the pH smoothly decreases with time. However, there does appear to be a slight plateau that could be due to a second stage reaction.

It has been reported (IV.1.7) that K_{sp} for ferrous hydroxide is about 10^{-14}. Using this K_{sp}, one can calculate that the curve shown in Figure IV.1.5 should be expected. Thus,

$$K_{sp} = 10^{-14} = [Fe(II)][OH^-]^2 = [0.03][OH^-]^2 \qquad \text{[IV.1.2.]}$$

and

$$[OH^-] = \sim 5.8 \times 10^{-7}\ M/L \qquad \text{[IV.1.3.]}$$

The OH^- concentration due to dissociation of pure water is about 10^{-7}. Thus, the addition of 0.03M $Fe(OH)_2$ will only marginally increase the OH^- concentration over that of pure water. If the solubility is due to the equation

$$Fe(OH)_2 \rightleftharpoons FeOH^+ + OH^- \qquad \text{[IV.1.4.]}$$

the contribution of the iron compound to the concentration of OH^- will be even less. It is therefore reasonable that there should be little deviation from the curve expected for the addition of sulfuric acid to pure water.

The X-ray diffraction pattern of the green solid collected at the end of the first oxidation stage, but while the pH was still 8.0, is shown in Figure IV.1.6. The pattern contains strong peaks at 2Θ = 8, 16 and 24 degrees, which corresponds to the [00Z] reflection of Green Rust (II), where Z is 1, 2, or 3 (IV.1.6). The green intermediate in the solid state appears to be less readily oxidized than it is in an aqueous suspension since the change in color and XRD pattern was not observed until the solid was exposed to air for 40 minutes.

The crystalline phase detected in the product collected following the completion of oxidation corresponding to the end of the second stage is γ-FeOOH with only trace amounts of α-FeOOH. The XRD pattern in Figure IV.1.7, with the five most intense peaks at 2θ ~14, 27, 36 , 47 and 56 degrees, is that expected for γ-FeOOH.

A pH curve with respect to time of oxidation is presented in Figure IV.1.8. Before the oxidation, the suspension pH was 8.12. As oxygen was added to the suspension, the pH remained constant for about 37 minutes. After 37 minutes, the pH suddenly dropped from 8.2 to 7 within 4-5 minutes. Thereafter, the pH of the suspension slowly decreased from 7 to 6. After 87 minutes, the pH suddenly decreased to 4. During the course of the oxidation of $Fe(OH)_2$, eight samples were collected for characterization at the times shown in Figure IV.1.8. A comparison of this curve with the one in Figure IV.1.1 shows that the oxidation of the $Fe(OH)_2$ suspension represents reproducible chemical reactions. Their X-ray diffraction patterns are presented in Figure IV.1.9 and a determination of their crystal structure by transmission electron microscopy (TEM) is reported in the following paper (IV.1.8). These samples are described in detail as follows.

Sample 1 was taken before oxidation. The whitish solid rapidly turned dark brown when it contacted air. An attempt to obtain an X-ray pattern for the white solid failed because it was too air sensitive.

Sample 2 was taken at 13 minutes when the suspension pH was 8.04. The solid was green. Like sample 1, it was also very air sensitive and the XRD pattern that was recorded was probably not representative of the initial sample.

Sample 3 was dark green. When withdrawn from the suspension at 37 minutes, the pH was 8.2. The solid appeared to be less air sensitive than samples 1 and 2 since its color did not change significantly when it was exposed to air for at least 40 minutes during the X-ray determination. About 31% of the total iron in this solid was Fe(III), and the X-ray diffraction data agreed closely with that of Green Rust (II).

Sample 4 was blue. It was collected at 48 minutes when the suspension pH was 6.7. Like sample 3, it was stable when it contacted with air for 40 minutes, but it slowly turned to yellow. About 40% of the total iron in the solid was Fe(III). The X-ray diffraction pattern shows that this sample was Green Rust (II), with some Fe_3O_4.

Sample 5 was dark green, and was obtained after the oxidation had proceeded for 67 minutes with a suspension pH of 6.5. About 60% of the total iron was Fe(III). The X-ray diffraction data indicate that the major component of the solid was Fe_3O_4 with small amounts of γ-FeOOH and α-FeOOH; Green Rust (II) was not detected in the XRD pattern for this solid.

Sample 6 was taken at 87 minutes when the suspension pH was 6.1. The XRD pattern for the greenish yellow solid consisted of peaks corresponding to γ-FeOOH

with small amounts of Fe_3O_4 and α-FeOOH. About 80% of the total iron in the solid was Fe(III).

Sample 7 was taken at 107 minutes when the suspension pH was 4.1. The solid was orange-yellow and was identified by the X-ray diffraction pattern as γ-FeOOH with small amounts of α-FeOOH. Fe_3O_4 was not observed in the solid. Fe(II) in this solid was too low to be detected by the titration technique.

Sample 8, withdrawn at 150 minutes, was orange-yellow. XRD data showed that the product was γ-FeOOH with small amounts of α-FeOOH.

The molar fraction of ferrous iron, Fe(II) %, in each of these suspensions (including both the solid phase and the suspension) was determined by titration. A plot of Fe(II) % versus reaction time (Figure IV.1.10) shows that Fe(II) % in the suspension decreases linearly with time until about 80% of Fe(II) is oxidized. The amount of the Fe(III) formed with time indicates that all of the oxygen added was utilized to oxidize Fe(II); the lack of a detectable flow of oxygen exiting the reactor until about 80 mole % of the Fe(II) was converted is consistent with this.

The molar fraction of ferrous iron in the solid phase was also determined by titration. The Fe(II) in the solid phase is not linear with time, but shows a slight deviation (Figure IV.1.10).

The Fe(II) concentration in the supernatant liquid in contact with each solid was determined. Fe(III) was not detected by titration of the supernatant liquid. The Fe(II) concentration in the solution changed with time as presented in Figure IV.1.11. The iron concentration in the supernatant liquid before the oxidation is determined to be 0.0365 M/L by the titration; it should be 0.0314 M/L based upon the Fe/OH ratio and

the solubility product. The initial Fe(II) in solution is thus within 2.3% of the expected value. As Fe(III) is produced the concentration of Fe(II) in solution decreases to a minimum value of about 0.009 M/L. This minimum does not occur at the point where the pH abruptly changes but appears to occur at a point where both TEM (IV.1.8) and XRD indicate the presence of both GRII and Fe_3O_4. Thus, it appears that the formation of GRII causes about 40% of the Fe(II) not initially precipitated as $Fe(OH)_2$ to be precipitated as GRII. The decrease in pH produces a further decrease in the Fe(II) and both the TEM and XRD indicate that the decrease from about 37 minutes to 48 minutes is due to the conversion of some of the iron present as GRII to Fe_3O_4. This presumably occurs through the conversion of Fe(II) in GRII to Fe(III) and at the same time releasing additional Fe(III); at least a portion of the Fe(III) formed during the period from 37 to 48 minutes precipitates as Fe_3O_4 rather than α-FeOOH or γ-FeOOH. As the oxidation of Fe(II) continues, both GRII and Fe_3O_4 are converted, either through dissolution/reprecipitation reactions or solid state reactions, to γ-FeOOH. Finally, when the suspension pH has decreased to 3.8, oxidation is slow so that the final solution contains the same Fe(II) concentration as was present in the suspension at the beginning of the oxidation.

IV.1.4.a. Mass Balance

To confirm our titration data, mass balance calculations were made. The calculations are based on the fact that the added oxygen reacted completely with ferrous hydroxide until all of the Fe(II) initially present as $Fe(OH)_2$ had been oxidized. The calculations are described below.

The molar fraction of Fe(III) can be calculated from the amount of oxygen added since oxygen completely reacted with Fe(II) hydroxide:

$$4Fe(OH)_2 + O_2 \rightarrow 4FeOOH + 2H_2O \qquad [IV.1.5]$$

The amount of oxygen added was calculated from oxygen flow rate (18.5 mL/min.) and time (min.). The data are listed in Table IV.1.1.

The molar fraction of Fe(II) in solution was calculated from data for the titration of the filtrate obtained from each of the samples:

Fraction of Fe(II) in liquid =

(conc. of Fe(II) in the filtrate)/(conc. of Fe(total)) **[IV.1.6]**

The concentration of Fe(total) is 0.22M. The data for the molar fraction of Fe(II) in the solution are given in Table IV.1.2.

Finally, the molar fraction of Fe(II) in the solid phase can be calculated using the equation:

M.F. of Fe(II) in solid phase = 1-[M.F. of Fe(II) in solution] -

[M.F. of Fe(III) (total)] **[IV.1.7]**

where M.F. is the molar fraction.

The data for the molar fraction of Fe(II) in solid phase are collected in Table IV.1.3. Figures IV.1.12 and IV.1.13 illustrate that the data calculated from the mass balances are consistent with the titration data.

The molar fractions of Fe(II) and Fe(III), based on the mass balance calculation data, in the suspension are shown in Figure IV.1.14. In Figure IV.1.14, curve A represents the molar fraction change with time for Fe(II) in the supernatant liquid; curve B represents the molar fraction change with time for Fe(II) in the solid

phase; and curve C represents the molar fraction change with time for Fe(III) in the suspension.

IV.1.5. DISCUSSION

In the present experiment, the molar ratio of [Fe(II)] : [OH^-] was 0.5833 (7/12). Thus, the initial reaction can be described as follows:

$$7\,FeSO_4 + 12\,NaOH \rightarrow 6\,Fe(OH)_2 + 6\,Na_2SO_4 + Fe(II) + SO_4^{2-} \quad \text{[IV.1.8.]}$$

Under this condition, essentially all of the added OH^- are consumed to form $Fe(OH)_2$, and 1/7th of the Fe(II) remains in solution. Because the added base is consumed in the precipitation process, the suspension is only slightly basic (pH = 8.2).

As oxygen is passed through the suspension, ferrous ions in the solution are oxidized to produce ferric ions which combine with ferrous ions to form an iron mixed-valence green complex. It has been reported (IV.1.9) that the green complex consists of Fe(II)-O-Fe(III), which exhibits a charge transfer absorption band at 337 nm due to the oxo-bridges. The soluble green complex has been proposed to have the empirical formula $[(Fe(II))_2(Fe(III))(OH^-)_4(O^{2-})]^+$ (IV.1.10). The green rust has been viewed to have limited solubility and to precipitate during the first stage, incorporating sulfate ion for charge balance. This intermediate is oxidized further to produce γ-FeOOH during the second stage. At the end of first stage, $Fe(OH)_2$ has been completely converted to Green Rust(II) at a pH 8.0. Thus, the molar fraction of Fe(III) in Green Rust(II) is estimated to be about 30 per cent. The suggested chemical formula, which was based upon Mössbauer data and chemical analysis, is $4Fe(OH)_2 \bullet 2FeOOH \bullet FeSO_4 \cdot nH_2O$

(IV.1.1,IV.1.10). The percentage of Fe(III) calculated from the amount of oxygen consumed agrees with the amount expected for this formula.

For such a complex situation one could envision a large number of oxidation-reduction schemes. Standard reduction potentials of oxygen in acid (pH = 0) and alkaline (pH = 14) solutions are listed in Table IV.1.4 together with the reduction potentials for pH = 8.2 and 6.5, the pH for the first and second stage reactions respectively (IV.1.11). The reduction potential can be calculated from

$$E/volt = E^{o} + 0.05916 \log H^{+}(mol/L) P_{O_2}(atm)^{1/2} \qquad [IV.1.9.]$$

The reduction potentials of the couples O_2/H_2O and H^+/H_2 as a function of pH are illustrated in Figure IV.1.15. In theory, the solvent should be oxidized to O_2 when the reduction potential is greater than the solid line in Figure IV.1.15. Actually, kinetic effects may require a greater potential than represented by the solid line. The broken line in Figure IV.1.15 represents this kinetic effect by estimating that the overpotential to account for kinetic effects is 0.5V. Thus, in practical cases oxygen (or hydrogen) formation is better represented by the broken line.

Peroxide is involved in several reactions listed in the acidic reactions of Table IV.1.4. This provides a complication since H_2O_2 can act as both an oxidizing and reducing agent. Thus, many materials are effective for the catalytic decomposition of peroxide. This decomposition can be viewed as an oxidation-reduction process and most homogeneous catalysts are oxidation-reduction couples of which the oxidizing agent can oxidize (be reduced by) H_2O_2 and the reducing agent can reduce (be oxidized by) H_2O_2. The data in Table IV.1.4 indicate that any complex with a

reduction potential in acid between 0.695 and +1.776 should catalyze the reaction. For the couple Fe(III)/Fe(II), E° is +0.771V; therefore, a mixture of Fe(II) and Fe(III) should catalyze the decomposition of peroxide, and it does. Thus:

$$2Fe(III) + H_2O_2 \xrightarrow{-2H^+} 2Fe(II) + O_2 \qquad \text{[IV.1.10.]}$$

$$2Fe(II) + H_2O_2 \xrightarrow{+2H^+} 2Fe(III) + 2H_2O \qquad \text{[IV.1.11.]}$$

$$NET: \; 2H_2O_2 \rightarrow 2H_2O + O_2 \qquad \text{[IV.1.12.]}$$

Considering the equations and the corresponding emf at a pH of about 8.2, where the green rust is formed during the first stage of the oxidation, it appears that the sequence of reactions listed below is most reasonable:

$$O_2 \xrightarrow{+e^-} O_2^- \xrightarrow{+H_2O,\, e^-} HO_2^- + OH^-$$
$$HO_2^- \xrightarrow{+H_2O,\, 2e^-} 3OH^- \qquad \text{[IV.1.13]}$$

and the net reaction for reduction is

$$O_2 + 2H_2O + 4e^- \rightarrow 4OH^- \qquad \text{[IV.1.14.]}$$

Fe(II) is oxidized, and then undergoes hydrolysis:

$$Fe(OH)_2 \rightarrow Fe(OH)_2^+ + e^- \qquad \text{[IV.1.15.]}$$

$$Fe(OH)_2^+ + H_2O \rightarrow Fe(OH)_3 + H^+ \qquad \text{[IV.1.16.]}$$

For this consideration it does not matter whether we write the Fe(III) species as $Fe(OH)_3$ or a decomposition product, FeOOH (+ H_2O). Thus, the net reaction for oxidation at pH = 8.2 is

$$4Fe(OH)_2 + 2H_2O + O_2 \rightarrow 4Fe(OH)_3 \qquad \text{[IV.1.17.]}$$

During the first stage, the $Fe(OH)_3$ species does not remain but further reacts to dehydrate and/or then to produce green rust:

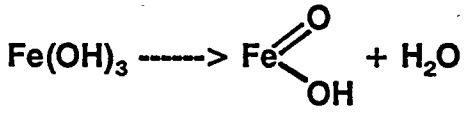

[IV.1.18]

This Fe(III) species is probably not completely formed but rather reacts with Fe(II) species to form a complex that can formally be described as:

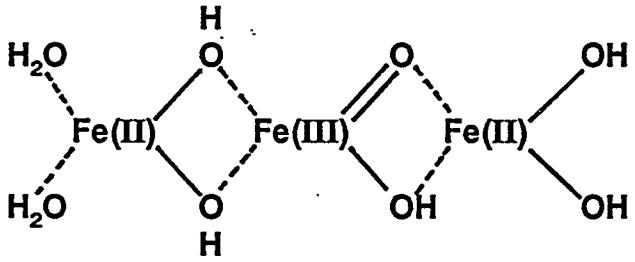

[IV.1.19]

Combining two of the above species would provide a possible structure for green rust (IV.1.1,IV.1.11):

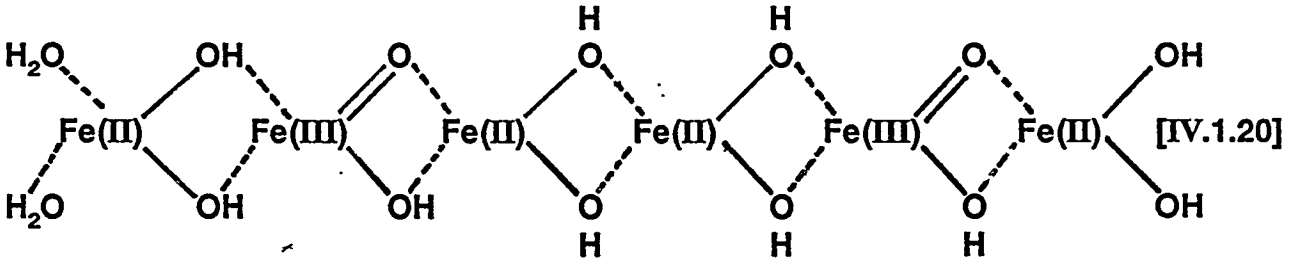

[IV.1.20]

The above equations ([IV.1.14] and [IV.1.17]) cannot explain why there should be a rapid decrease in the pH at the completion of the first stage. However, the pH certainly does decrease, and it decreases in a similar manner when Fe(III) is added as when oxidation continues. It appears that the first step change in pH is a result of the relative kinetics of H^+ generation and consumption together with a change in the reaction pathway for oxygen. The following is taken as evidence to support the view that in a slightly basic solution the reaction that generates H^+ is much more rapid than the reaction(s) that consume it:

1. When oxygen flow is temporarily stopped there is a gradual increase in pH, and not the abrupt change as noted with pH decrease.
2. When an OH^- containing solution is added to the suspension there is nearly an instantaneous increase in the pH, unlike the slow increase noted when oxygen flow is stopped.
3. Following addition of OH^- and continued oxygen flow there is a rapid decrease in pH to attain the value that existed prior to OH^- addition.
4. The addition of Fe(III) causes a rapid decrease in pH.

Thus, at or near the completion of the formation of Green Rust, the situation resembles that shown in Figure IV.1.5.

One explanation is that the more rapid reaction (production of H^+ in contrast to the slower series reaction leading to OH^-) produces an excess of H^+ sufficient to cause a decrease in pH to effectively stop the formation of the final product, OH^-, and

to effect a change in the reaction pathways for reduction of the oxygen. It is speculated that as the pH decreases the intermediate in the basic reduction, HO_2^-, is converted to H_2O_2, and then to water, rather than to OH^- as was the case in the basic media.

Another possibility is that as long as there is an excess of solid Fe(II), the precipitation of Fe(III) and Fe(II) as Green Rust allows the two reaction couples to produce H^+ and OH^- in equal amounts. Upon depletion of most of the Fe(II) it is possible that the Fe(III) species, following hydrolysis to formally produce $Fe(OH)_3 + H^+$, undergoes dimerization, etc. that produces additional H^+.

Another possibility is that the oxidation of the $FeSO_4$, and 1/7th of the initial Fe(II) is present as $FeSO_4$, begins with the depletion of the $Fe(OH)_2$ through partial oxidation and combination of the Fe(II) and Fe(III) to form Green Rust. Thus, if this is the case, the hydrolysis of the resulting Fe(III) would produce a proton for each $FeSO_4$ that is oxidized. Only an insignificant amount of the $FeSO_4$ present in the 0.2M Fe suspension would have to be oxidized to decrease the pH from about 8 to 6.5; at a pH = 6.5 the oxidation of Green Rust becomes responsible for the consumption of oxygen and the pH remains essentially constant during the second stage. Upon completion of oxidation of the Fe(II) present in Green Rust at the completion of the second stage, the oxidation of $FeSO_4$ again takes place with a resulting decrease in pH until such a low pH is attained that oxidation will essentially cease. Whether one of these, or some other reaction, is responsible for the sudden step change in pH, it is

an experimental fact that the pH does decrease and that oxidation of the Green Rust intermediate occurs at approximately pH = 6.2

The oxidation processes for low concentrations of iron in neutral or slightly acidic media using oxygen has been studied extensively (for example, IV.1.12-IV.1.19). Goto (IV.1.13), for example, proposed that the following reactions are involved in this oxidation:

$$Fe(II) + O_2 \rightarrow Fe(III) + O_2^- \qquad \text{[IV.1.21.]}$$

$$O_2^- + H^+ \rightarrow HO_2 \qquad \text{[IV.1.22.]}$$

$$Fe(II) + HO_2 \rightarrow Fe(III) + HO_2^- \qquad \text{[IV.1.23.]}$$

$$H^+ + HO_2^- \rightarrow H_2O_2 \qquad \text{[IV.1.24.]}$$

$$Fe(II) + H_2O_2 \rightarrow Fe(III) + OH^- + OH\cdot \qquad \text{[IV.1.25.]}$$

$$Fe(II) + OH\cdot \rightarrow Fe(III) + OH^- \qquad \text{[IV.1.26.]}$$

$$Fe(III) + 3H_2O \rightarrow Fe(OH)_3 + 3H^+ \qquad \text{[IV.1.27.]}$$

Globally, it has been shown (IV.1.17-IV.1.19) that the stoichiometry describing the oxidation of Fe(II) to Fe(III) and it subsequent hydrolysis is described as:

$$4Fe(II) + 10H_2O + O_2 \rightarrow 4Fe(OH)_3 + 8H^+ \qquad \text{[IV.1.28.]}$$

While this net reaction may account for dilute Fe(II) salt solutions such as $FeSO_4$, and even for the dilute solutions as used for generating the data in Figure IV.1.5, it cannot

account for the case of $Fe(OH)_2$ oxidation as represented in Figure IV.1.1. In this case we have

$$4Fe(OH)_2 + 2H_2O + O_2 \rightarrow 4Fe(OH)_3 \qquad \textbf{[IV.1.29.]}$$

and the pH of the solution will remain constant.

Thus, based on the reactions proposed by Goto (IV.1.13), one possible pathway is:

Oxidation

$$4H_2O + 4Fe(OH)_2 \rightarrow 4Fe(OH)_3 + 4H^+ + 4e^- \qquad \textbf{[IV.1.30.]}$$

Reduction

$$\begin{aligned} O_2 + 2e^- &\rightarrow O_2^{2-} \\ O_2^{2-} + 2H^+ &\rightarrow H_2O_2 \\ H_2O_2 + e^- &\rightarrow OH^- + OH\cdot \\ OH\cdot + e^- &\rightarrow OH^- \\ 2OH^- + 2H^+ &\rightarrow 2H_2O \end{aligned} \qquad \textbf{[IV.1.31.]}$$

$$NET \quad O_2 + 4e^- + 4H^+ \rightarrow 2H_2O \qquad \textbf{[IV.1.32.]}$$

Combining the oxidation and reduction equations provides one of the possible global equations for the oxidation process that occurs during the constant pH portion that constitutes the second stage.

$$O_2 + 2H_2O + 4Fe(OH)_2 \rightarrow 4Fe(OH)_3 \qquad \textbf{[IV.1.33.]}$$

In principle, the oxidation of $Fe(OH)_2$ by the above reaction could be effected in the solid state; however, it appears that the indirect reaction is not only faster but is able

to selectively form the uniform green rust species wherein the arrangements of the Fe(III) and Fe(II) ions in the same in each unit.

The above reaction scheme cannot describe all oxidations of Fe(II) by oxygen. The reactions are applicable, however, for a suspension that has [Fe]/[OH] ~ 0.58 as was the case for this particular investigation.

In neutral solutions (pH ~7), Fe_3O_4 is formed, presumably via Green Rust (II) by further oxidations. Bernal et al. (IV.1.6) suggested that Fe_3O_4 is formed near the surface of the particle of Green Rust (II) by the coprecipitation of ferrous ion with ferric iron. Our results show that the concentration of Fe(II) in the supernatant was decreased during the formation of Fe_3O_4; however, other mechanisms are also consistent with this observation.

It is surprising that further oxidation of Fe_3O_4 produces γ-FeOOH. We are unaware of any report on the formation of γ-FeOOH through Fe_3O_4 by oxidation. It is known that oxidation of Fe_3O_4 may take place upon the dissolution of the ferrous ions or upon the adsorption of the oxygen on the Fe_3O_4 particles. In either case, the iron ions should diffuse toward the surface of Fe_3O_4 particles, thus causing oxidation (IV.1.5). When Fe_3O_4 is oxidized to γ-FeOOH, the OH groups must be introduced into Fe_3O_4 particles. Hence, this solid state oxidation seems to be very difficult. The fact that the concentration of Fe(II) in the supernatant increased during the oxidation of Fe_3O_4 indicate that a dissolution/reprecipitation process is likely to be involved during the formation of γ-FeOOH.

It is well known that Green Rust can be produced as an intermediate during the oxidations of $Fe(OH)_2$. In spite of the many studies (IV.1.20) on this green material; its composition remains unknown. Hush (IV.1.21) reported that the absorption band at 337 nm in the greenish-blue material obtained by partial oxidation of $Fe(OH)_2$ had a maximum intensity of absorbance when the Fe(III)/Fe(II) ratio was about 1/1. Kiyama (IV.1.22) found from chemical analysis and Mössbauer effect measurement that the Green Rust formed in a sulfate solution containing about 40% of Fe(III) and the ratio of Fe(III)/Fe(II) in Green Rust (II) never exceeded 1/1. Feitknecht and Keller (IV.1.20a) obtained a green compound that contained about 28% Fe(III). Olowe and Gémin (IV.1.23) suggested that ratio of Fe(II)/Fe(II) is 2.5. Tamaura et al. (IV.1.24) obtained a value 2 for the Fe(II):Fe(III) ratio. These results are in good agreement with our estimate of the Fe(III) content in Green Rust to be in a range of 30~40%.

IV.1.6. ACKNOWLEDGMENT

This work was supported by DOE contract #DE-AC22-90PC90056 and the Commonwealth of Kentucky.

IV.1.7. REFERENCES

IV.1.1. Olowe, A. A.; Pauron, B.; Genin, J. M. R. *Corrosion Science*, **1991**, *32*, 985.

IV.1.2. Kiyama, M.; Jikuhara, N.; Takada, T. *Bull. Chem. Soc. Japan*, **1973**, *46*, 323.

IV.1.3. Kiyama, M.; Takada, T. *Bull. Chem. Soc. Japan*, **1972**, *45*, 1923.

IV.1.4. Kiyama, M.; Akita, T.; Shimizu, S.; Okuda, Y.; Takada, T. *Bull. Chem. Soc.*, **1972**, *45*, 3422.

IV.1.5. Kiyama, M. *Bull. Chem. Soc. Japan*, **1974**, *47*, 1646.

IV.1.6. Bernal, J. D.; Dusyputa, E. R.; Marckay, A. L. *Clay. Min. Bull.*, **1959**, *4*, IV.1.15.

IV.1.7. Greenwood, N. N.; Ernshaw, A. "Chemistry of the Elements", Pergamon Press, Oxford, 1984, pg 1269.

IV.1.8. Srinivasan, R.; Lin, R.; Spicer, R. L.; Davis, B. H. submitted.

IV.1.9. Misawa, T.; Hashimoto, K.; Suetaka, W.; Shimodaira, S. *J. Inorg. Nucl. Chem.*, **1974**, *35*, 4159.

IV.1.10. Barton, T. F.; Price, T.; Dillars, J. G. *J. Coll. & Interface Sci.*, **1991**, *141*, 553.

IV.1.11. Greenwood, N. N.; Ernshaw, A. "Chemistry of the Elements", Pergamon Press, Oxford, 1984, pg 736.

IV.1.12. Tamara, H.; Goto, K.; Nagayama, M. *J. Inorg. Nucl. Chem.*, **1976**, *38*, 113.

IV.1.13. Goto, K.; Tamara, H.; Nagayama, M. *J. Inorg. Chem.*, **1970**, *9*, 963.

IV.1.14. Weiss, J. *Naturwissenschaften*, **1935**, *23*, 64.

IV.1.15. Haber, F.; Weiss, J. *Proc. Roy. Soc. (London)*, **1934**, *A147*, 332.

IV.1.16. Burb, G. W.; Baxendale, J. H.; Geoge, P.; Hargrave, K. R. *Trans. Faraday Soc.*, **1957**, *47*, 462.

IV.1.17. Just, G. Z. *J. Phys. Chem.*, **1908**, *63*, 385.

IV.1.18. Halide, J.; Eberhardt, M. *Vom Wasser*, **1957**, *79*, 24.

IV.1.19. Stumm, W.; Lee, G. F. *Ind. Eng. Chem.*, **1961**, *53*, 143.

IV.1.20. (a) Feitkecht, W.; Keller, G. *Z. Anorg. Chem.*, **1950**, *262*, 61; (b) Gancedo, J. R.; Martinez, M. L.; Oton, J. M. *Anal. Quim.*, **1983**, *79*, 470; (c) Stamph, P. P. *Corrosion Sci.*, **1969**, *9*, 185; (d) Vins, J.; Subrt, J.; Zapletal, V.; Hanousek, F. *Collect. Czech. Chem. Comm.*, **1987**, *52*, 93.

IV.1.21. Hush, N. S. "Progress in Inorganic Chemistry", Vol. 8, p 391.

IV.1.22. Kiyama, M. *Bull. Inst. Chem. Res.*, **1969**, *47*, 607.

IV.1.23. Olowe, A. A.; Génin, J. M. R. *Corrosion Sci.*, **1991**, *32*, 965.

IV.1.24. Tamaura, T.; Yoshida, T.; Katsura, T. *Bull. Chem. Soc. Jpn.*, **1984**, *57*, 2411.

Table IV.1.1
Calculation of Fe(III) from Oxygen Flow Rates (0.360 mmole total iron)

Time Period (Min.)	O_2 Added during the Period (mL)	Fe(III) produced by the oxidation (mmole)	Fe(III) (total) (mmole)	Molar Fraction of Fe(III) calculated from Col. 4	Molar Fraction of Fe(III) obtained from titration
0	0	0	0	0.00	0.00
0-13	241	0.043	0.043	0.12	0.09
14-37	444	0.079	0.122	0.34	0.30
38-48	204	0.036	0.158	0.44	0.41
49-67	352	0.063	0.221	0.61	0.59
68-87	370	0.066	0.287	0.80	0.79

Table IV.1.2

Molar Fraction of Fe(II) in Solution (Fe(total) = 0.22M/L)

Time (Min.)	Concentration of Fe(II) in the Solution (M/L)	Molar Fraction of Fe(II) in Solution (M/L)
0	0.0360	0.16
13	0.0330	0.15
37	0.0220	0.10
48	0.0088	0.04
67	0.0242	0 11
87	0.0360	0.16

Table IV.1.3
Molar Fractions of Fe(II) in the Solid Phase

Time Period (Min.)	Molar fraction of Fe(III) in Solution	Molar Fraction of Fe(II) in Liquid Phase	Molar Fraction of Fe(II) in Solid Phase	Fe(II) % in Solid Phase Calculated from Cols. 2 and 4	Fe(II) % in Solid Phase Obtained from Titration Data
0	0	0.16	0.84	100	100
13	0.12	0.15	0.73	86	---
37	0.34	0.10	0.56	62	60
48	0.44	0.04	0.52	54	53
67	0.61	0.11	0.28	31	27
87	0.80	0.16	0.04	5	4

Table IV.1.4

Standard Reduction Potentials for Oxygen in Acid and Basic Solution and Reduction Potentials at pH 6.5 and 8.2

Reaction	E°	pH	
Acidic		6.5	8.2
$O_2 + 4H^+ + 4e^- \rightleftarrows 2H_2O$	1.229	0.8445	0.7439
$O_2 + 2H^+ + 2e^- \rightleftarrows H_2O_2$	0.695	0.311	0.210
$O_2 + H^+ + e^- \rightleftarrows HO_2$	-0.105	-0.490	-0.590
$H_2O_2 + H^+ + e^- \rightleftarrows H_2O_2$	1.495	1.111	0.626
$H_2O_2 + 2H^+ + 2e^- \rightleftarrows 2HO_2$	1.776	1.39	1.29
$H_2O_2 + H^+ + e^- \rightleftarrows OH + H_2O$	0.71	0.326	0.225
$OH + H^+ + e^- \rightleftarrows H_2O$	2.85	2.47	2.37
Basic			
$O_2 + 2H_2O + 4e^- \rightleftarrows 4OH^-$	0.401	0.845	0.7441
$O_2 + H_2O + 2e\text{-} \rightleftarrows HO_2^- + OH^-$	-0.076	0.309	0.409
$O_2 + e \rightleftarrows O_2^-$	-0.563	-0.119	-0.220
$O_2^- + H_2O + e \rightleftarrows HO_2^- + OH^-$	0.413	0.857	0.756
$HO_2^- + H_2O + 2e^- \rightleftarrows 3OH^-$	0.878	1.32	1.22
$HO_2^- + H_2O + e \rightleftarrows OH + 2OH^-$	-0.245	0.199	0.098
$OH + e^- \rightleftarrows OH^-$	2.02	2.46	2.36

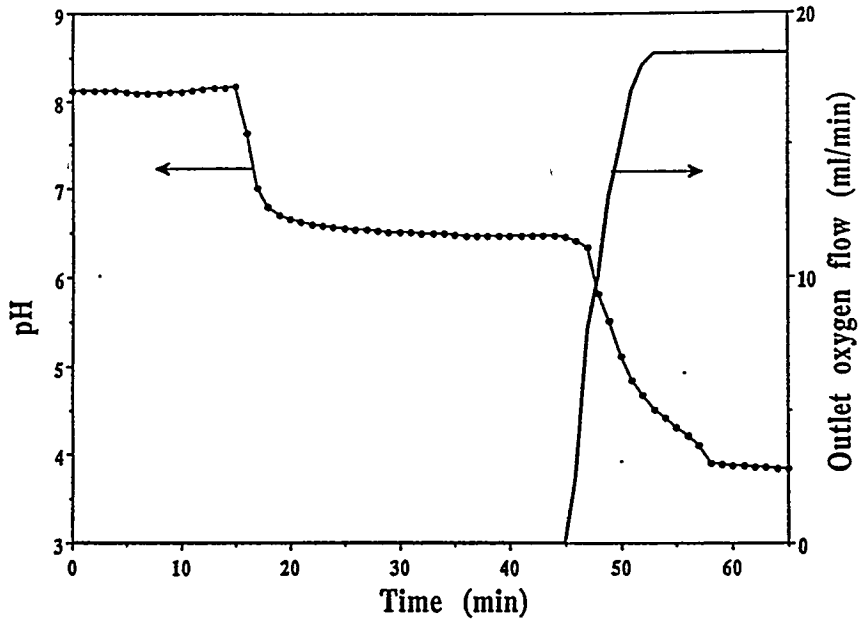

Figure IV.1.1. Recorded variation of the pH of the suspension and the outlet oxygen flow with respect time for the oxidation of Fe(II) (inlet oxygen flow, 18.5 mL/min.; initial $Fe(II)/OH^- = 0.5883$).

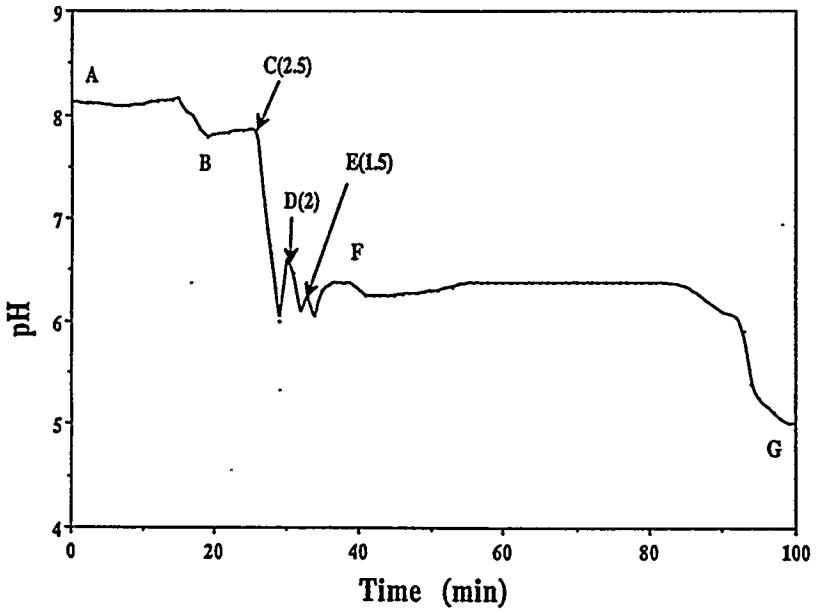

Figure IV.1.2. Recorded variation of the pH of the suspension with respect to reaction time for Fe(II) oxidation (during A → B and F → G oxygen was added; during B → C and E → F oxygen flow was stopped; at C, D and E, 2M ferric sulfate was added (number in parenthesis is the mL added; initial conditions as in Figure 1).

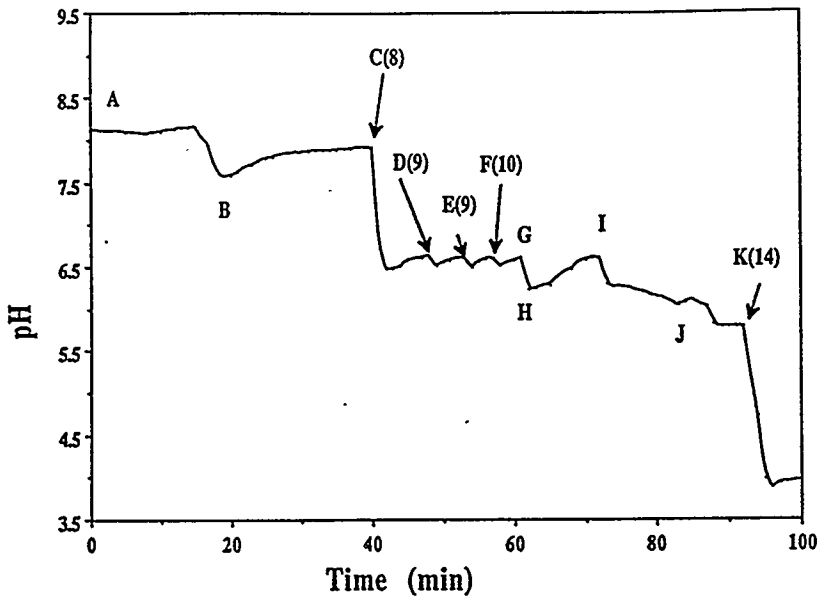

Figure IV.1.3. Recorded variation of the pH of the suspension with respect to oxidation time (during A → B and G → H oxygen was flowing; during B → C, H → I and J → K oxygen flow was stopped; at C, D, E, and F, K, 2N H_2SO_4 was added (number in parenthesis is the mL added) with nitrogen flow; initial conditions as in Figure 1).

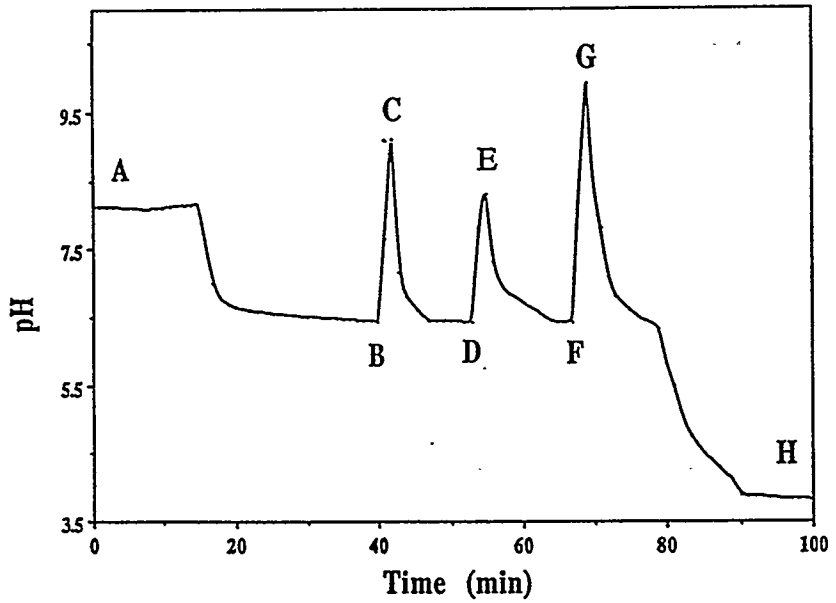

Figure IV.1.4. Recorded variation of the pH of the suspension with respect to time (during A → B, C → D, E → F, and G → H oxygen was flowing; at B, D, and F, 1M NaOH (number in parenthesis is the mL added was added while oxygen was flowing; initial conditions as in Figure 1).

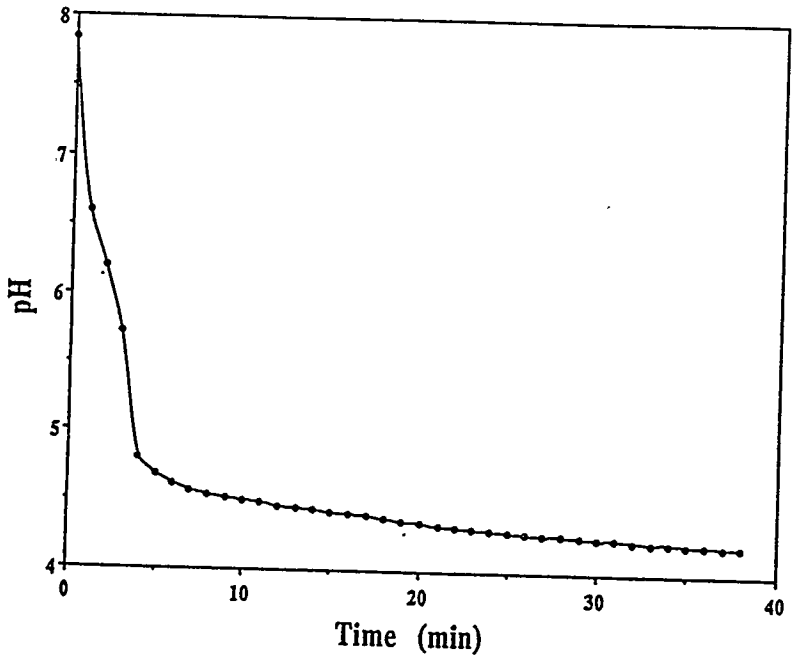

Figure IV.1.5. Recorded variation of the pH with respect to oxidation time ([Fe(II)] = 0.029 M).

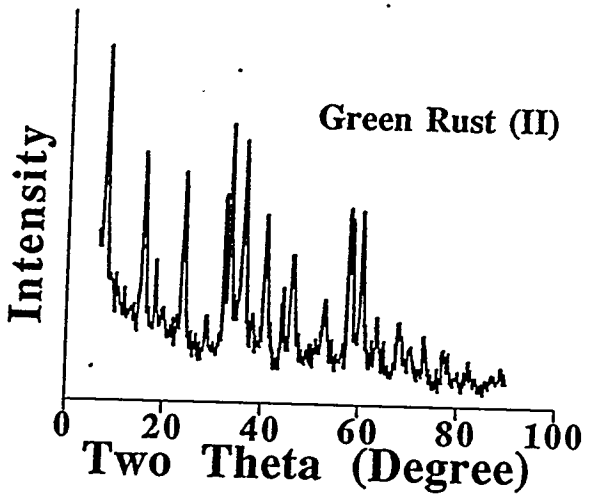

Figure IV.1.6. The X-ray diffraction pattern of Green Rust (II).

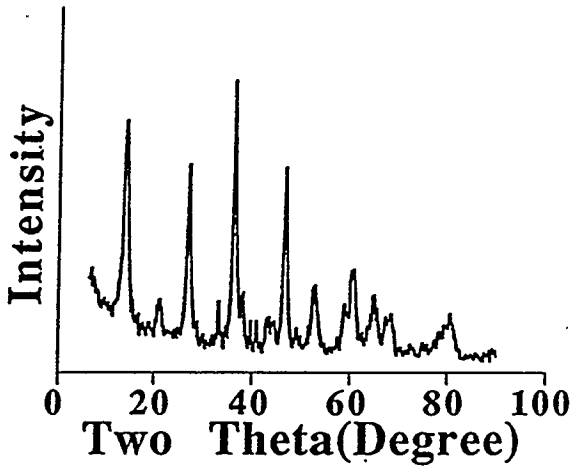

Figure IV.1.7. The X-ray diffraction pattern of γ-FeOOH.

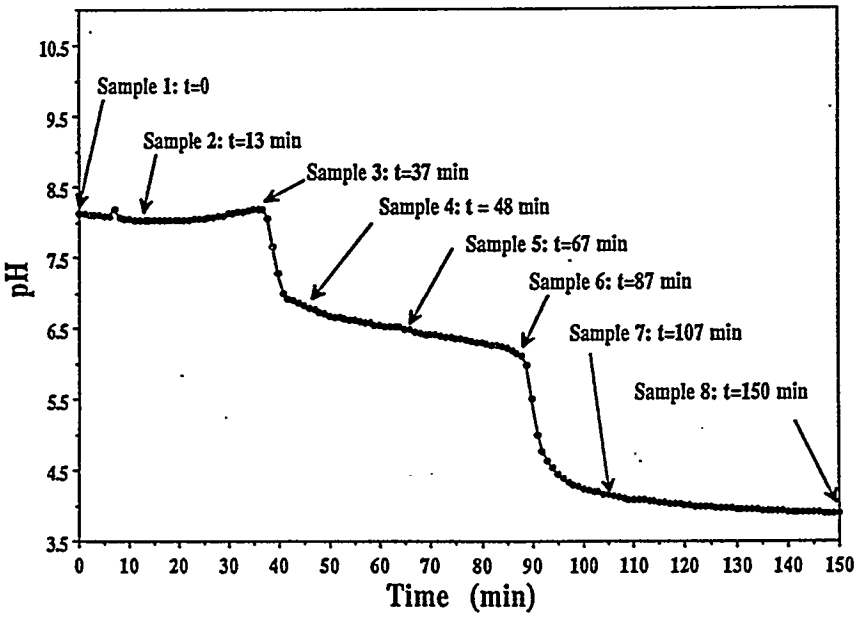

Figure IV.1.8. The change in the pH of a $Fe(OH)_2$ with oxidation time (sample collection times are indicated).

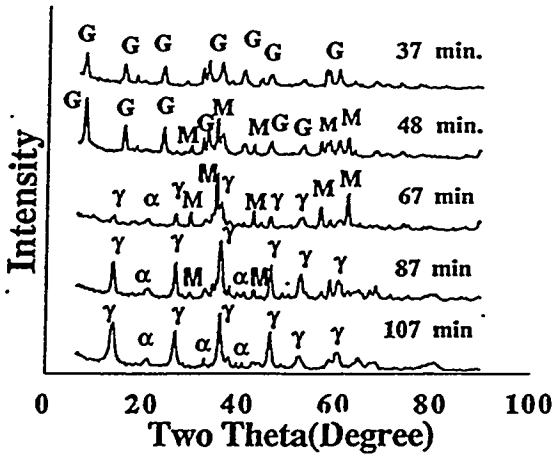

Figure IV.1.9. The X-ray diffraction pattern for samples withdrawn at the times indicated in Figure 8. The times in the figure are the time when the sample was withdrawn; the peaks are identified as: G, GR(II); M, Fe_3O_4; α, α-FeOOH, and γ, γ-FeOOH.

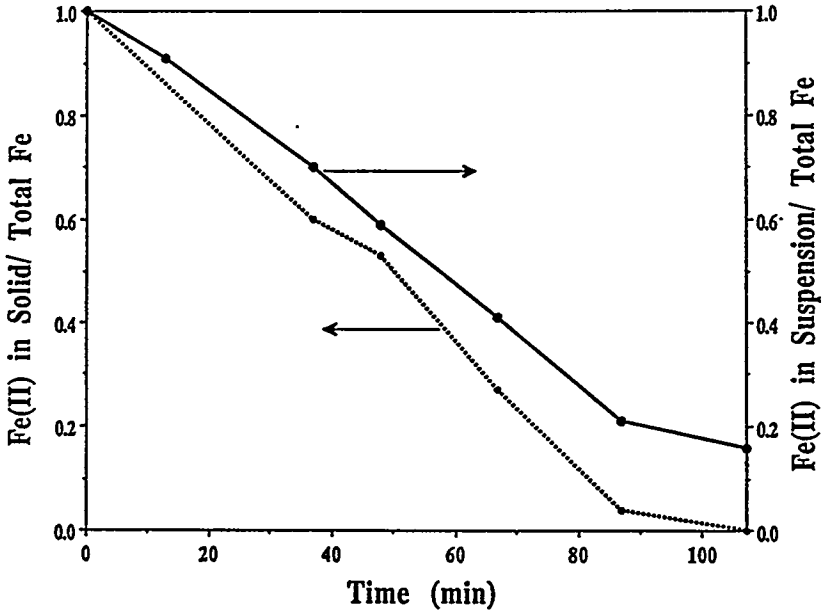

Figure IV.1.10. Changes of the Fe(II) percentage with time for the total suspension and the solid sample as a function of oxidation time.

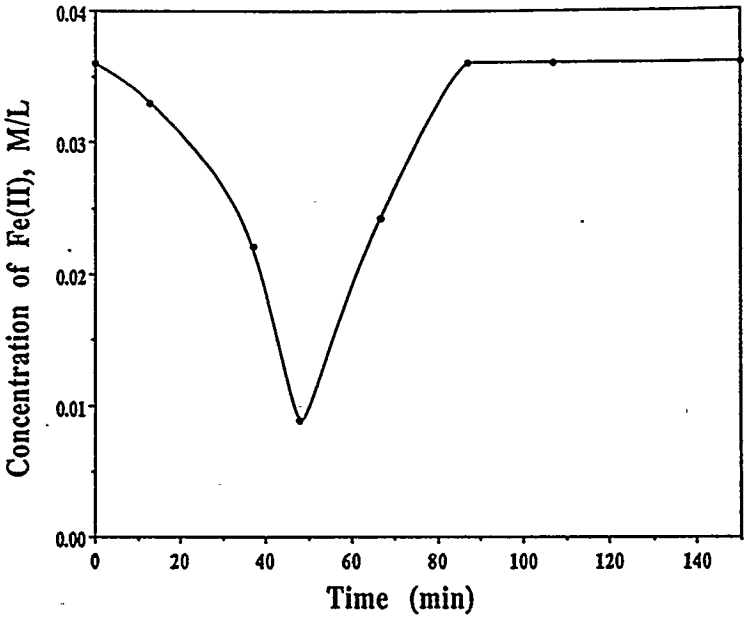

Figure IV.1.11. The concentration of Fe(II) in the supernatant liquid versus oxidation time.

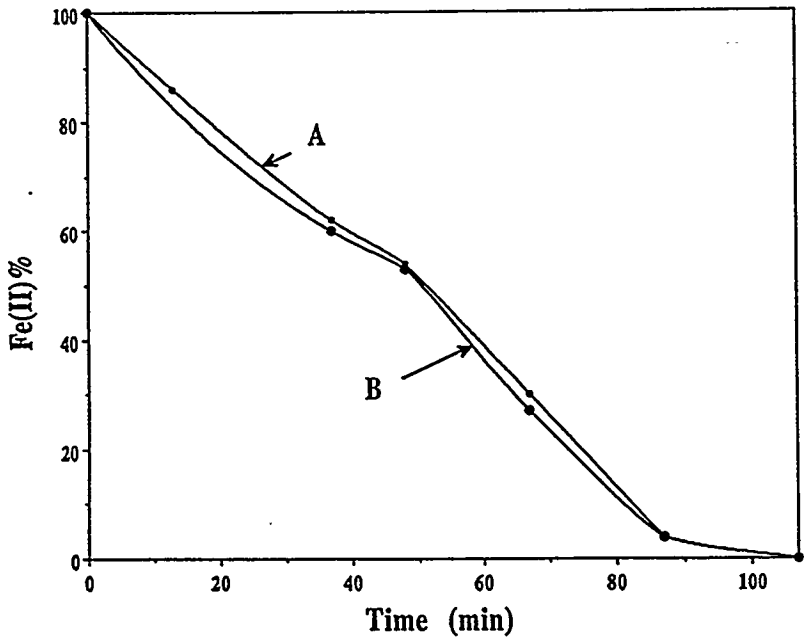

Figure IV.1.12. Comparison of the Fe(II) percentage in the solid phase obtained from mass balance calculations based upon oxygen flow (A) with those based on the titration data (B).

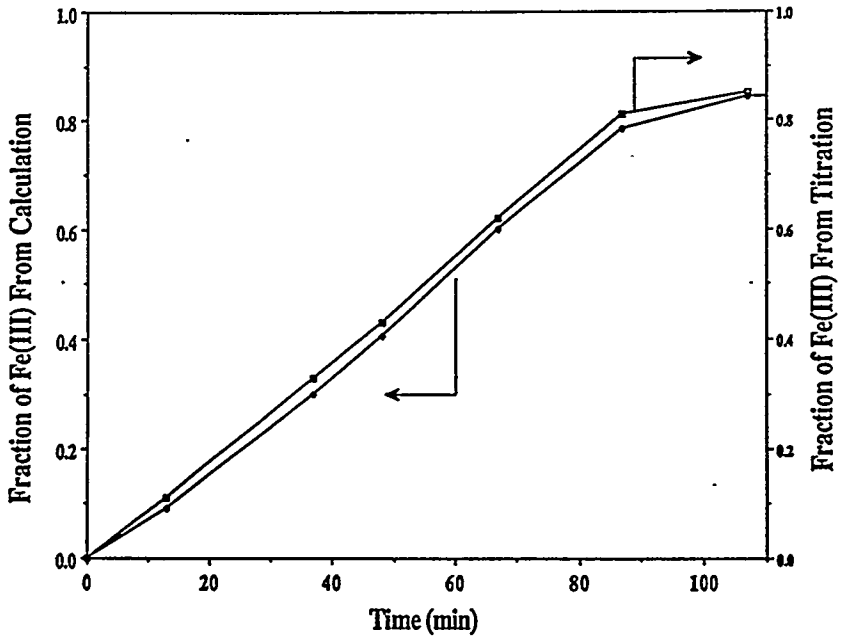

Figure IV.1.13. Comparison of the molar fraction of Fe(III) obtained by calculations based on oxygen flow and the titration data.

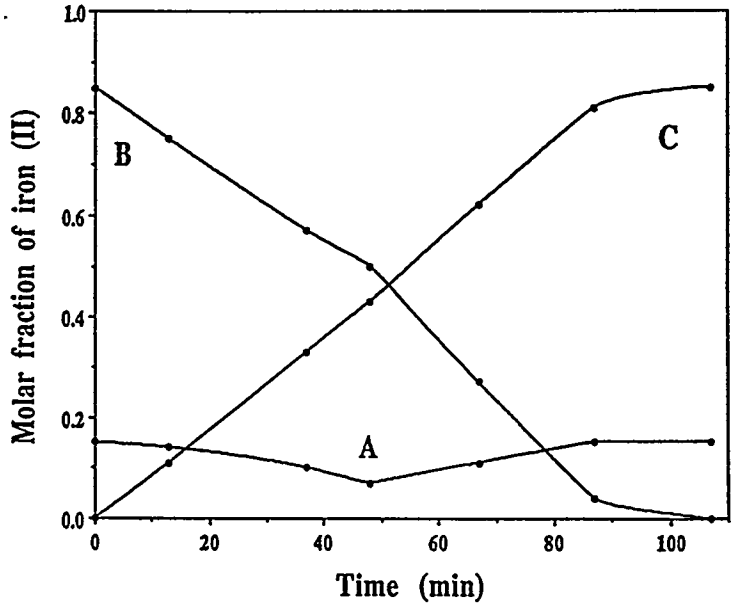

Figure IV.1.14. Molar fraction of Fe(II) and Fe(III) in the solid and liquid phases versus time of oxidation plots (A, molar fraction of Fe(II) in liquid phase; B, molar fraction Fe(II) in solid phase, and C, molar fraction of Fe(III) in solid).

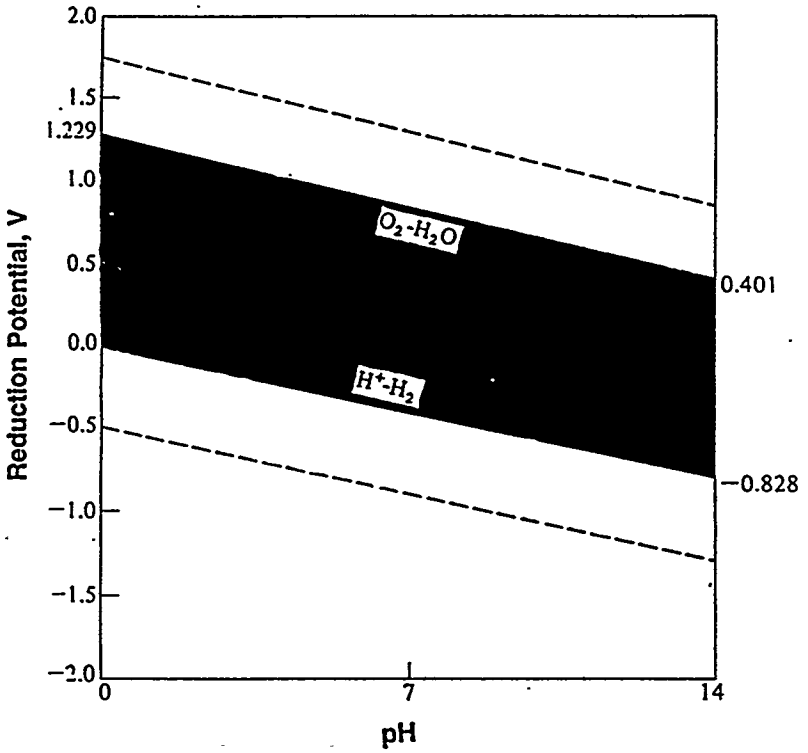

Figure IV.1.15. Variation of the reduction potentials of the couples O_2/H_2 and H^+/H_2 as a function of pH (boundaries of the black zone). The broken lines lie 0.5V above and below the reduction potential lines and give an approximation of the practical limits of oxidants and reductants in aqueous solution beyond which the solvent itself is oxidized to $O_2(g)$ or reduced to $H_2(g)$.